American Journal of Condensed Matter Physics 2012, 2(1): 1-10
DOI: 10.5923/j.ajcmp.20120201.01

Computational Investigation of Electronic and Optical Properties of Si, Ge and $Si_{1-x}Ge_x$ Alloys Using the FP-LMTO Method Augmented by a Plane-Wave Basis

K. Zellat[1], B. Soudini[1,*], N. Sekkal[2] , S. M. Ait Cheikh[3]

[1]Applied Materials Laboratory (AML), University of Sidi Bel Abbès, Sidi Bel Abbès, 22000, Algeria
[2]Département de Physique-Chimie, Ecole Normale Supérieure de l'Enseignement Technique, Oran, 31000, Algeria
[3]Lab. de Dispositifs de Communication Conversion Photovoltaique , Ecole Nationale Polytechnique, Alger, Algeria

Abstract An investigation into the structural, electronic and optical properties of Si, Ge, and $Si_{1-x}Ge_x$ for different compositions was conducted using first-principles calculations based on density functional theory (DFT). The total energies were calculated within the full -potential linear muffin-tin orbital (FP-LMTO) method augmented by a plane-wave basis (PLW), implemented in Lmtar code. The effects of the approximations to the exchange-correlation energy were treated by the local density approximation (LDA). From our simulation results, it is found that the theoretical ground-state parameters, the band structure, the density of states (DOS), the chemical bonding and the optical properties agree well with the experiment and other theoretical calculations. The accuracies found from the present calculations allow us to describe the properties of the electronic as well as the optoelectronic devices based on the $Si_{1-x}Ge_x$ alloy.

Keywords FP-LMTO Calculation, Electronic Properties, Optical Properties, $Si_{1-X}ge_x$ Alloy

1. Introduction

Semiconductors have played a major role in the current technological revolution. For the past years, a major aspiration of condensed matter physics has been to explain and predict the properties of solids knowing only the identities of the constituent atoms. Recently, this goal has been realized for many semiconductors properties. The successes are best illustrated by the progress made in understanding the structural, electronic and optical properties of semiconductors.

Among semiconductors, the covalent semiconductors Si and Ge have been studied extensively both theoretically and experimentally[1,2]

Group IV semiconductor alloy like Si-Ge, have the immense potential for technological applications[3-5].

Silicon Germanium ($Si_{1-x}Ge_x$) alloy is good candidate as a substitute material for Si in low-power and high-speed semiconductor device technologies[6]. Optoelectronic devices, such as heterojunction bipolar transistors, are already in industrial production. $Si_{1-x}Ge_x$ is also promising as alloying material for quantum well devices, for the 1.3-1.55 μm optical communication detectors[7,8] for the 2 μm to 12 μm infrared detectors[9,10], and modulation-doped field-effect transistors[11]. The main reason for this is the requirement of the direct gap materials for fabrication of optoelectronic devices. The system, for example, Si-Ge improves the transport and optical properties as compared to silicon. Due to such applications of the system in optoelectronics devices, the theoretical and experimental studies of Si-Ge system is an important task. The number of bonding electrons does not change when the solid solution of Si1−xGex is formed and, hence, the theoretical study of the system of Si-Ge solid solutions is also interesting.

Although much efforts have been paid on the growth of $Si_{1-x}Ge_x$ and $Si_{1-x}Ge_x$ /Si as well on electrical characterization, there is still a lack of information about the optical properties of $Si_{1-x}Ge_x$. This prompts us to study these proprieties in the present work.

The main goal of this paper is to provide a consistent and complete set of electronic and optical parameters that are need for our next quantitative calculations of the quantum cascade laser (QCL) properties based on these materials.

This paper is organized as follows. In Section 2 we describe the theoretical methodology of the first principles calculations and discuss the details of the calculations. The results of the band structure, the density of states (DOS), the chemical bonding and the optical properties are presented and discussed in Sec. 3. Finally, Section 4 summarizes the paper.

2. Method of Calculations

* Corresponding author:
sba_soudini@yahoo.fr (B. Soudini)
Published online at http://journal.sapub.org/ajcmp

In this work, full potential linear muffin -tin orbital (FP-LMTO) method, as employed in the lmtart code[12-14], has been applied to perform first -principles total energy calculations. It's a specific implementation of density functional theory within the local density approximation (LDA). In this method, there is no shape approximation to the crystal potential, unlike methods based on the atomic-spheres approximation (ASA) where the potential is assumed to be spherically symmetric around each atom. For mathematical convenience the crystal is divided up into regions inside muffin-tin spheres, where Schrödinger's equation is solved numerically, and an interstitial region.

In all LMTO methods the wave functions in the interstitial region are Hankel functions. Each basis function consists of a numerical solution inside a muffin-tin sphere matched with value and slope to a Hankel function tail at the sphere boundary. The so-called multiple-kappa basis is composed of two or three sets of s, p, d, etc. LMTOs per atom. The extra variational degrees of freedom provided by this larger basis allow for an accurate treatment of the potential in the interstitial region. One advantage of this method over, pseudopotential-based methods, in the context of high-pressure physics and elsewhere, is that the core and semi-core electrons are explicitly included in the calculations. In addition, to first order all materials require equal computational effort, with no dependence on a deep versus shallow pseudopotential. However, pseudopotential based methods are generally much more computationally efficient for large numbers of atoms, due in part to a simpler mathematical foundation that is more amenable to clever algorithmic shortcuts.

In order to solve the Kohn-Sham (KS) equation, the wave function needs to be expanded in a known basis set {χ} in the following form:

$$|\psi\rangle = \sum_{i=1}^{N} ci|\chi\rangle \tag{1}$$

Operators are then treated as matrices and functions as vectors on a computer. The Kohn-Sham equation can then be transformed to a general eigenvalue problem:

$$(H - \varepsilon(k)O)c = 0 \tag{2}$$

Where c is the vector of {ci} and H and O are the Hamiltonian and overlap matrices respectively with matrix elements:

$$\{H\}ij = \langle \chi i|H|\chi j\rangle$$
$$\{O\}ij = \langle \chi i|\chi J\rangle \tag{3}$$

The eigenvalue problem and calculation of matrix elements are the most time consuming parts in the self-consistent cycle and therefore needs to be implemented in an efficient way.

A very important consequence of the translational periodicity of an infinite crystal is that the basis set can be written as a Bloch sum:

$$\chi(k,r) = \sum_{T}^{\infty} e^{ikT}\chi i(r - T)) \tag{4}$$

Where *T* is a primitive translation vector and *k* is a vector in the reciprocal space. This means that in order to obtain the wave function in the entire space, the KS-equation needs to be solved only for a selected number of k-points lying inside the Brillouin zone (BZ). The equations can be solved separately and independently for each k-point, through an integration over the Brillouin zone is necessary in the end to obtain the band energy.

The chosen basis set $\{\chi_i\}$ needs on one hand to be mathematically simple to simplify the calculation of matrix elements and on the other hand it needs to be suitable to the problem of interest to reduce the number of basis functions. In 1975, Andersen[15] constructed a basis set of *linear-muffin-tin-orbitals (LMTO)*, which are very well adapted to the crystal problem. It is a minimal basis set which reduces the size of the Hamiltonian matrix that in turn reduces the computational effort.

The starting point is to approximate the full crystal potential with a muffin-tin potential *VMT*. Then, we obtain a spherically symmetric potential well with radius *S* near the atomic site and a flat potential outside (interstitial):

$$V_{MT}(r) = \begin{cases} V(r) & r \le S \\ V_{MTZ} & r > S \end{cases}. \tag{5}$$

In the Atomic Sphere Approximation (ASA) the radius of the muffin-tin spheres S is chosen to be equal to the Weigner-Seitz radii S_{WS}. The muffin-tin spheres then overlap with each other and are space-filling, that is, the interstitial part of the crystal is neglected. Moreover, in the ASA the kinetic energy outside the muffin-tin sphere is chosen to be equal zero. If the crystal is not close-packed it is necessary to include so called *empty spheres* to reduce the overlap of muffin-tin spheres. To a first approximation, one can correct on ASA by adding some extra terms to the LMTO matrices, the so called *combined correction terms*[16].

In the muffin-tin geometry and after linearization of the solution to the radial Schrödinger (Dirac) equation inside the muffin-tin, the muffin-tin orbitals have the form[15,16].

$$\Psi_{lm}(r,E) \approx \begin{cases} \psi_{lm}(r) + (E - E_v)\psi_{lm}(r) & r \le S \\ K_{lm}(r)Y_{lm}(r) & r > S \end{cases}. \tag{6}$$

Here *Ev* is the linearization energy, K_{lm} (r) the irregular solution (Neumann function) to the Helmholtz equation outside the muffin-tin sphere, a function called envelope function and Y_{lm} are spherical harmonics. In order to have a smooth wave function, the solutions and their first derivative inside and outside the muffin-tin sphere are matched at the sphere boundary. The envelope function centered at a muffin-tin at *R* can be expressed inside a neighboring muffin-tin sphere at R' in terms of regular

Solutions (Bessel functions) $J_{l'm'}(r_{R'})$ as:(7)

$$K_{lm}(rR) = -\sum_{l'm'} S_{lml'm'} J_{l'm'}(rR') \tag{7}$$

Where $R \neq R'$ and $S_{lml'm'}$ are *structure constants* which only depend on crystal structure. It is possible by a transformation to screen the structure matrix and envelope function in order to minimize the overlap between different muffin-tin orbitals[17,18]. This representation is called *tight binding representation (TB)*[19]. Then, the LMTO-basis

can be used in the wave function expansion, Eq.1, and in the general eigenvalue problem, Eq.2, in order to obtain a solution to the one-particle Schrödinger equation. Alternatively, one could use the fact that all the tails from all other muffin-tin spheres must cancel inside a given muffin-tin sphere.

In order to achieve the energy eigenvalues convergence, the wave functions in the interstitial region were expanded in plane waves with a 63.549 Ryd energy cut-off and a number of plane waves equal to 9170. The charge density and the potential are represented inside the muffin-tin spheres (MTS) by spherical harmonics up to $l_{max} = 6$. The **k** integration over the Brillouin zone is performed up to (6, 6, 6) grid in the irreducible Brillouin Zone (BZ), using the tetrahedron method [20].

3. Results and Discussions

3.1. Electronic Band Structure of Si and Ge

Energy bands consisting of a large number of closely spaced energy levels exist in crystalline materials. The bands can be thought of as the collection of the individual energy levels of electrons surrounding each atom. The wavefunctions of the individual electrons, however, overlap with those of electrons confined to neighbouring atoms.

The Pauli Exclusion Principle does not allow the electron energy levels to be the same so that one obtains a set of closely spaced energy levels, forming an energy band. The energy band model is crucial to any detailed treatment of semiconductor devices. It provides the framework needed to understand the concept of an energy band gap and that of conduction in an almost filled band as described by the empty states. The energy band diagrams of semiconductors are rather complex[21].

The detailed energy band diagrams of silicon and germanium are shown in Figure 1.The energy is plotted as a function of the wavenumber, *k*, along the main crystallographic directions in the crystal, since the band diagram depends on the direction in the crystal. The energy band diagrams contain multiple completely-filled and completely-empty bands. In addition, there are multiple partially-filled band.

One can notice from the figure 1 that the smallest band gap of germanium and silicon are indirect, The values of these gaps turns out to be at 300K, 1.2eV and 0.661eV, respectively. At the same temperature, the energies corresponding to critical points for silicon are E_L=2.0eV, E_X= 1.2eV, $E_{\Gamma 1}$= 3.4eV. We have found an energy separation ($E_{\Gamma L}$ or $E_{\Gamma 2}$) equal to 4.2eV, and an energy spin-orbital splitting E_{so} equal to 0.044eV.

For the germanium at the same temperature, we have E_X =1.2eV, $E_{\Gamma 2}$=, 3.22eV, an energy separation ($E_{\Gamma 1}$, $\Delta E>$) = (0.8eV, 0.85eV) and an energy spin-orbital splitting E_{so} = 0.29eV.

With the LMTO (LPW) method, we found for Si, the values of muffin -tin spheres (MTS) , Spheres asa, Nrad= 2.221, 3.1823, 276 respectively . For Ge : MTS, Spheres asa, Nrad = 2.31, 3.3126, 3.32, respectively.

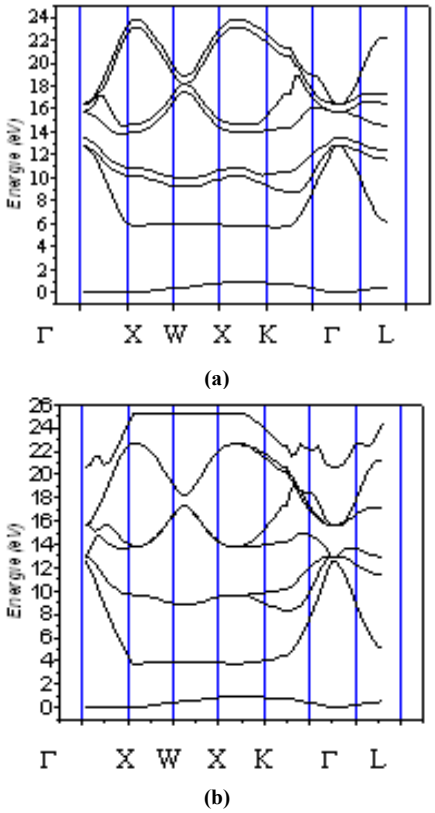

Figure 1. The calculated electronic energy-band structure of Si (a) and of Ge (b)

To have a depth insight of the origin of the different bands, one can plot the contribution from the different atomics orbital to the electronic energy band structure as shown in the Figure 2.

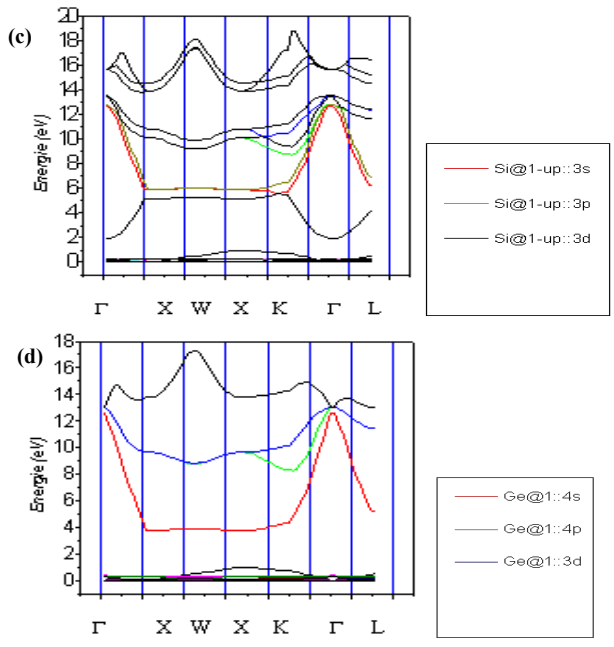

Figure 2. Contribution from the different atomics orbital to the electronic energy-band structure for Si (c) and for Ge (d)

3.2. Electronic Band Structure of the $Si_{1-x}Ge_x$ Alloy

The next step of our calculations is to show how the stochiometries could affect the band structure of the alloy based on the studied elemental semiconductors. The atom specific data of $Si_{1-x}Ge_x$ alloy are given in Table 1.

Table 1. The atom specific data of the $Si_{1-x}Ge_x$ alloy

Elements	Number of atoms	Lattice parameter in atomic units (A)	B over A ratio C over A ratio	Primitive translations in units of lattice parameter	Position of atom in the Unit cell in units of lattice parameter
$Si_{000}Ge_{100}$	8for Ge	10.04	1-1	1.0, 0.0, 0.0 0.0, 1.0, 0.0 0.0, 0.0, 1.0	0.0, 0.0, 0.0 1/4, 1/4, 1/4 1/2, 1/2, 0.0 3/4, 3/4, 1/4 0.0, 1/2, 1/2 1/4, 3/4, 3/4 1/2, 0.0, 1/2 3/4, 1/4, 3/4
$Si_{100}Ge_{000}$	8for Si				
$Si_{012}Ge_{087}$	1for Si, 7for Ge				
$Si_{087}Ge_{012}$	7for Si, 1for Ge				
$Si_{025}Ge_{075}$	2for Si, 6for Ge				
$Si_{075}Ge_{025}$	6for Si, 2for Ge				
$Si_{050}Ge_{050}$	4for Si, 4for Ge				
$Si_{037}Ge_{062}$	3for Si, 5for Ge				
$Si_{062}Ge_{037}$	5for Si, 3for Ge				

The detailed energy band diagrams of $Si_{1-x}Ge_x$ alloy are shown in Figure 3 (e_1, e_2, e_3, e_4) for $Si_{000}Ge_{100}$, $Si_{100}Ge_{000}$, $Si_{013}Ge_{087}$, and $Si_{088}Ge_{012}$, respectively.

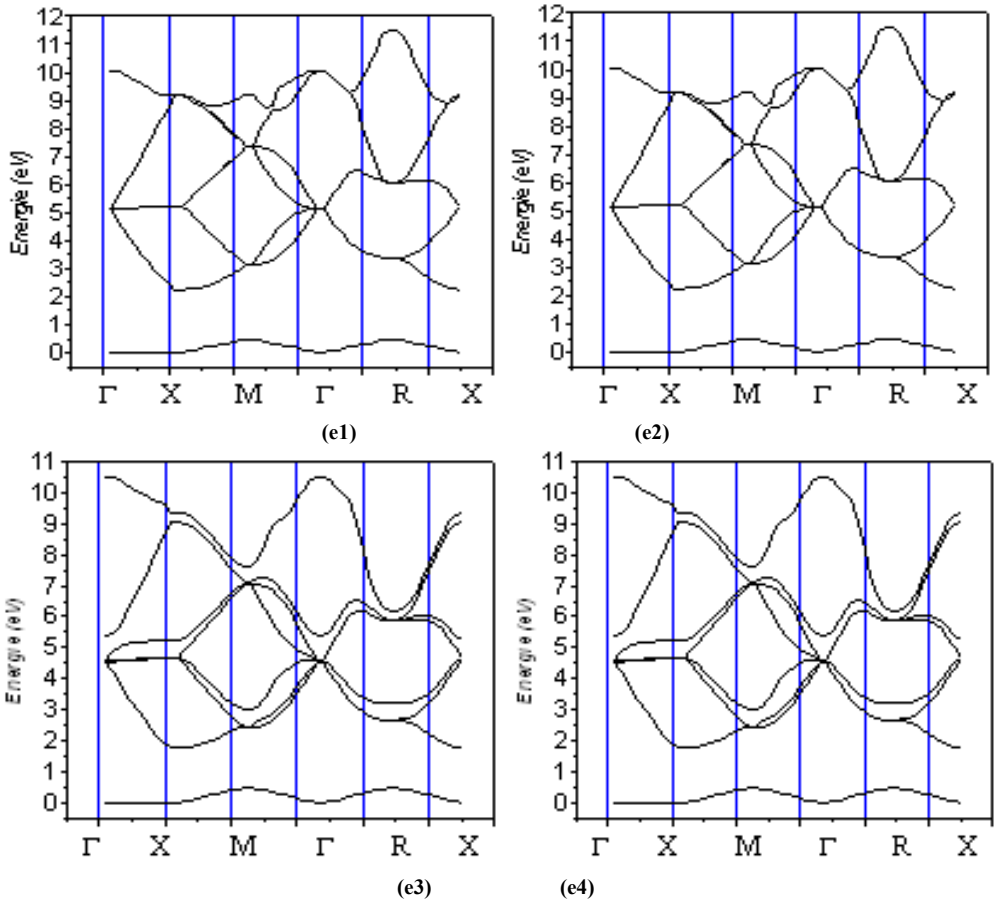

Figure 3. The calculated electronic energy-band structure of $Si_{1-x}Ge_x$ alloy for $Si_{000}Ge_{100}$ (e_1) , $Si_{100}Ge_{000}$ (e_2),, $Si_{013}Ge_{087}$ (e_3), and $Si_{088}Ge_{012}$ (e_4)

We show in figures 4 (f_1,f_2,f_3,f_4,f_5) the energy band diagrams of $Si_{025}Ge_{075}$, $Si_{075}Ge_{025}$, $Si_{050}Ge_{050}$, $Si_{038}Ge_{062}$, and $Si_{063}Ge_{037}$, respectively.

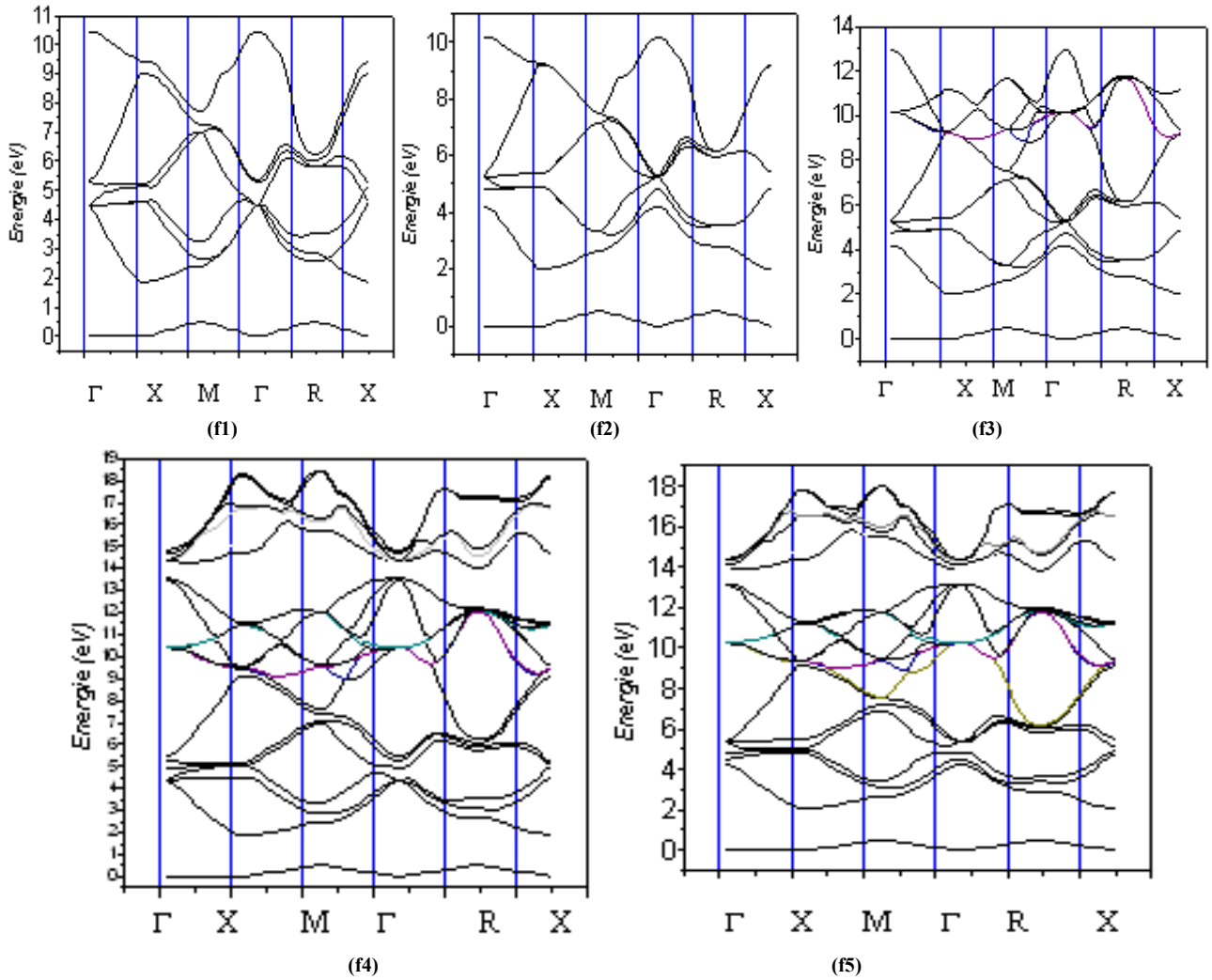

Figure 4. The calculated electronic energy-band structure of $Si_{1-x}Ge_x$ alloy for $Si_{025}Ge_{075}$ (f_1) , $Si_{075}Ge_{025}$ (f_2),, $Si_{050}Ge_{050}$ (f_3), $Si_{038}Ge_{062}$ (f_4) , and $Si_{063}Ge_{037}$ (f_5).

For the calculation of $Si_{1-x}Ge_x$ alloy we adopted a zinc-blend structure. The band structures of all the considered concentrations are for zinc-blend structure. Our results agree well with the self-consistent Full potential LMTO calculation of the band structure, especially for the minimum gap (near X point) and for the band ordering ($E_{g\Gamma\Gamma} > E_{g\Gamma L} > E_{g\Gamma X}$). The LDA energy band structures of Si_xGe_{1-x} alloys are found to be indirect for the zinc-blend structure. It is important to note that the band gap derived from LDA eigenvalues is too small; the LDA underestimates the band gaps. Thus, although the minimum gaps are brought close to experiments, the dispersion of the present band structure may not predict future experiments very well. These physical trends have been confirmed by other authors[22-24].

In this LDA, electronic properties are determined as functional of the electron density by applying local relations appropriate for a homogeneous electronic system. However, the experimental data of the principal energy gaps of $Si_{0.5}Ge_{0.5}$ alloy are not sufficiently available to allow an accurate determination of the potential parameters. To calculate the principal energy gaps for the zinc-blende structure of $Si_{1-x}Ge_x$ at 300 K for concentration $x < 0.85$, we have used the interpolation equation like $1.12-0.41x + 0.008x^2$ eV, but for $x > 0.85$ we have used the linear $1.86 - 1.2x$ eV. From these calculations one can state that the $Si_{1-x}Ge_x$ is a Si-like indirect semiconductor for $x < 0.85$ in good agreement with other results[25].

3.3. Electronic Charge Density of the $Si_{1-x}Ge_x$

To analyze the bonding properties, we have shown in Figure 5 ((1) and (2)) the electronic charge densities of Si and Ge, respectively.

It is well known that all properties of a microscopic system of N particles, e.g. charge densities can be obtained from the solution of Schrödinger's equation, but assuming a macroscopic crystal (N approx. 10^{24}) the equation can not be solved. Using the density functional theory of Kohn, and Sham[26,27], Schrödinger's equation can be transformed into a system of 10^{24} one-particle-equations, and each particle suffers from an effective potential $V_{eff}(r)$. Our calculation method LMTO is based on the Kohn-Sham theorem .

In figures 6 ((1) to (4)), we have illustrated the electronic charge densities of $Si_{000}Ge_{100}$, $Si_{100}Ge_{000}$, $Si_{050}Ge_{050}$, $Si_{037}Ge_{062}$ respectively. Using the other concentration (75%,

87%), we found the same graphs as for the $Si_{050}Ge_{050}$ alloy.

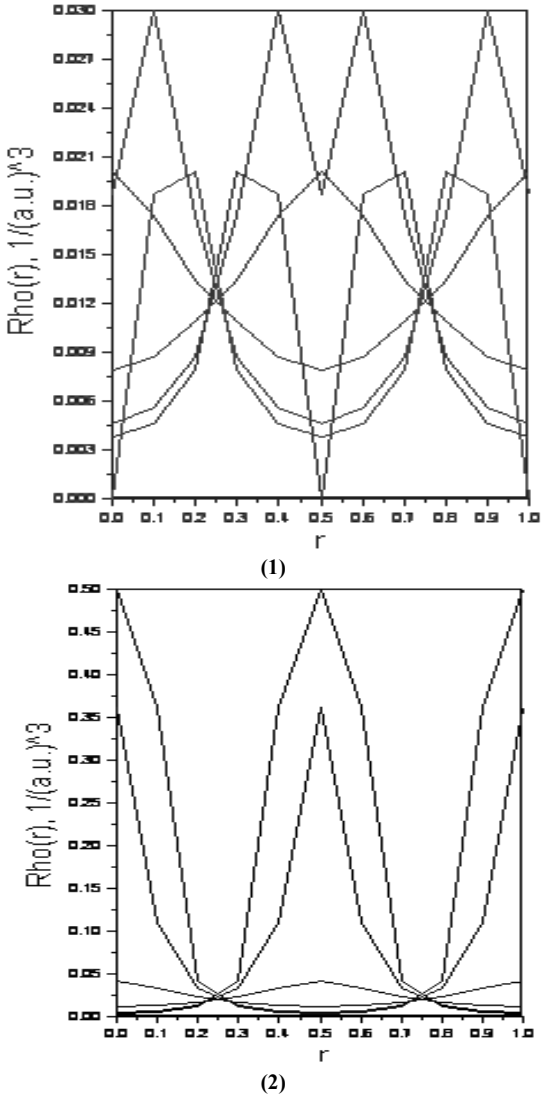

Figure 5. The calculated electronic charge densities of Si (1) and Ge (2)

The central feature of the calculated charge densities is the existence of pile up which indicating the covalent character of the bonds. To take into account the effect of the different values of composition,, found some different profiles of the charge densities. Since the total charge densities arise from the lowest valence band, the increase of the composition value leads to germanium profiles. This behaviour has been discussed by Philips [1].

3.4. Density of State of the $Si_{1-x}Ge_x$ Alloy

In statistical and condensed matter physics, the density of states (DOS) of a system describes the number of states at each energy level that are available to be occupied. A high DOS at a specific energy level means that there are many states available for occupation. A DOS of zero means that no states can be occupied at that energy level.

As was illustrated in Figure 7, the Fermi level is shifted to 0 eV. We show here the total DOS (sum of all basis which is considered in both atoms) that has considerable contribution towards total density of states. Our calculations for the total DOS of $Si_{000}Ge_{100}$ yield main structure at 17eV and 26eV above the Fermi level and for $Si_{050}Ge_{050}$ at11eVand 17eV, for $Si_{075}Ge_{025}$ at 12.5eV and 17 eV, $Si_{037}Ge_{062}$ at 11eV and 15.5eV, $Si_{087}Ge_{012}$ at 11eV and 15.5eV and 23eV above the Fermi level (See figures 5,6,7,8,9), respectively).

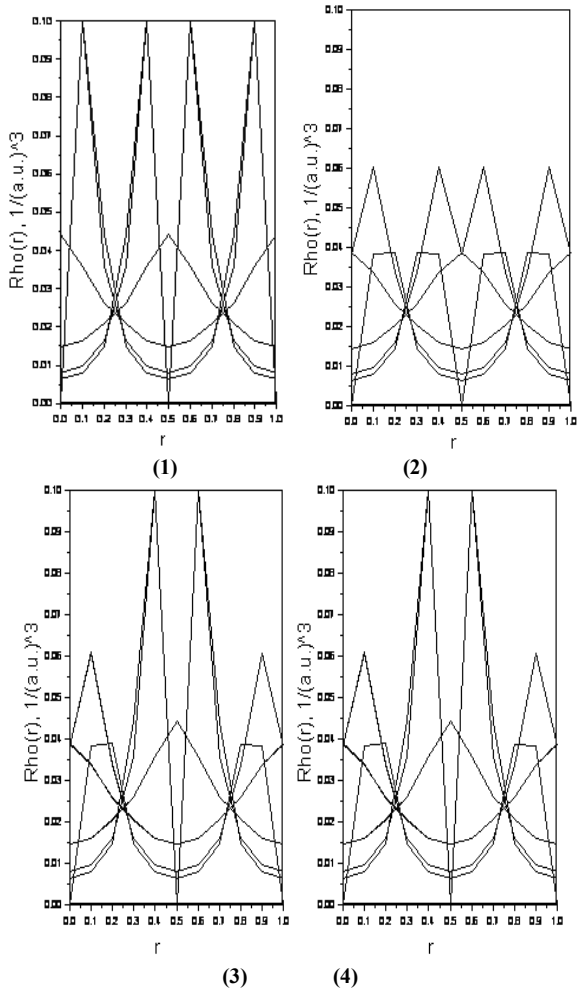

Figure 6. The calculated electronic charge densities of $Si_{000}Ge_{100}$ (1) , $Si_{100}Ge_{000}$ (2), $Si_{050}Ge_{050}$ (3), and $Si_{037}Ge_{062}$ (4)

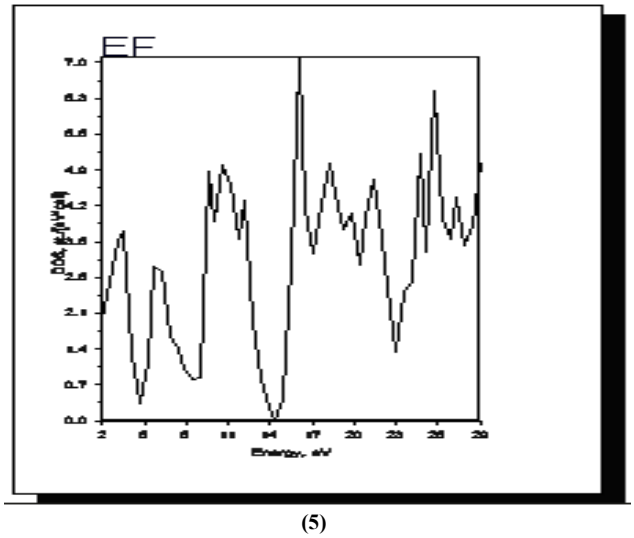

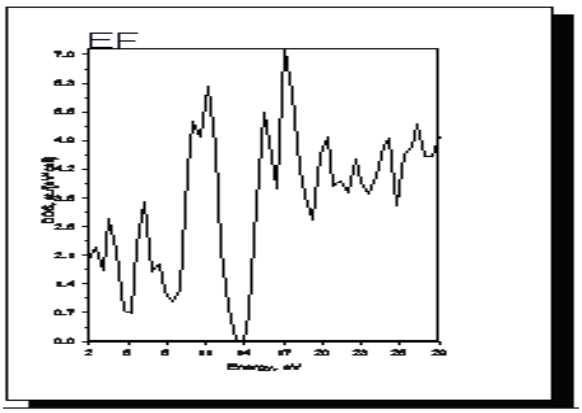

(6)

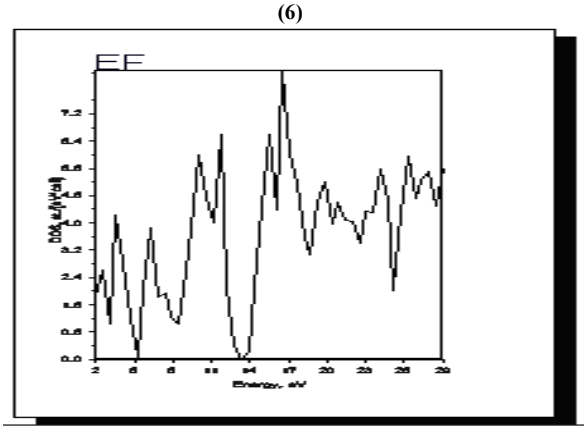

(7)

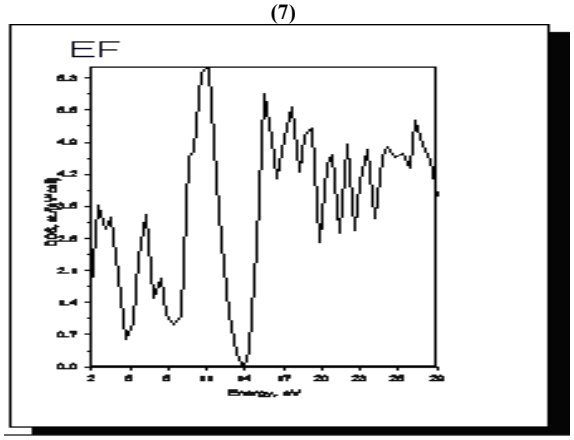

(8)

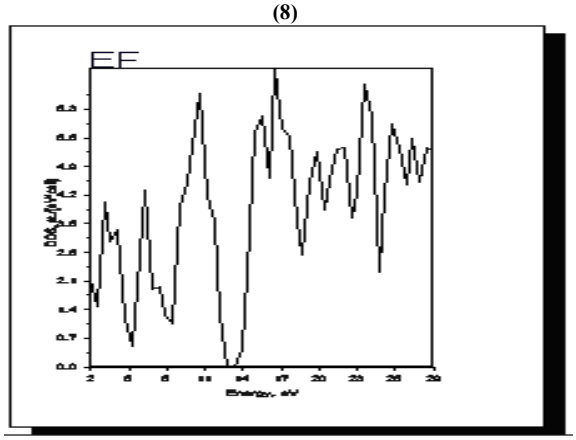

(9)

Figure 7. The calculated total DOS for $Si_{000}Ge_{100}$ (5), $Si_{050}Ge_{050}$ (6), $Si_{075}Ge_{025}$ (7), $Si_{037}Ge_{062}$ (8) and $Si_{087}Ge_{012}$ (9)

We can also state that the valence band density of states may be divided into three regions. Using the top of the valence band, the first region is predominately of s-like character stemming from the atomic 3s-states. The second region is a transition region with contribution from both s- and p-states. Finally, the last region is predominantly p-like. The feature which delineates these spectral regions is a sharp reduction or dip in the density of states compared to the average density.

The Contributions of different atomics orbitals to the DOS of Ge and $Si_{025}Ge_{075}$ are shown in Figure 8(10) and Figure 8(11). These profiles of the DOS confirm the above physical consideration and in the other hand agree well with others theoretical results[28].

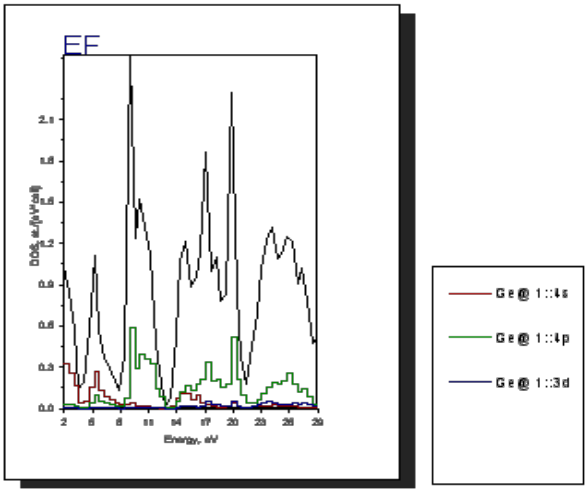

(10)

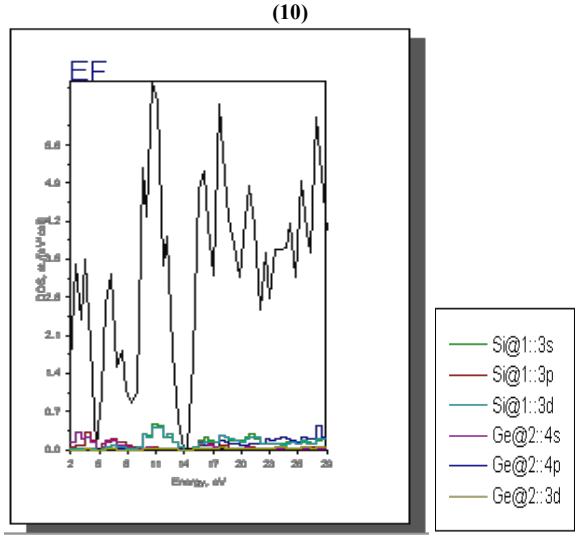

(11)

Figure 8. Contribution of different atomic orbital to the DOS for Ge (10) and for $Si_{025}Ge_{075}$ (11)

3.5. Optical Properties of the $Si_{1-x}Ge_x$ Alloy

It is well known that the basic optical properties of semiconductors result from the electronic excitation in crystals when an electromagnetic wave is incident on them. The calculation of the optical properties of the solids is beset with numerous problems. The knowledge of the dielectric func-

tions $\varepsilon(E)= \varepsilon_r(E)$-i$\varepsilon_i(E)$ allows to describe the optical properties of the medium at all phonon energies E.

Calculations of the dielectric function involve the energy eigenvalues and the electron wave functions. These are the natural output of the *ab initio* band structure calculation which is usually performed under local density approximation (LDA)[29,30] In the LMTO–LPW, we have calculated the frequency dependent imaginary dielectric function, real dielectric function, and electron energy loss spectrum. The effects of using *K* points in the BZ have already been discussed in the earlier work by Khan *et al* (1993) [31].

Before presenting the results for **$Si_{1-x}Ge_x$** alloy with different concentration, we will establish the reference of the optical results for Si and Ge. as depicted in Figure 9(12) and Figure 9(13), respectively.

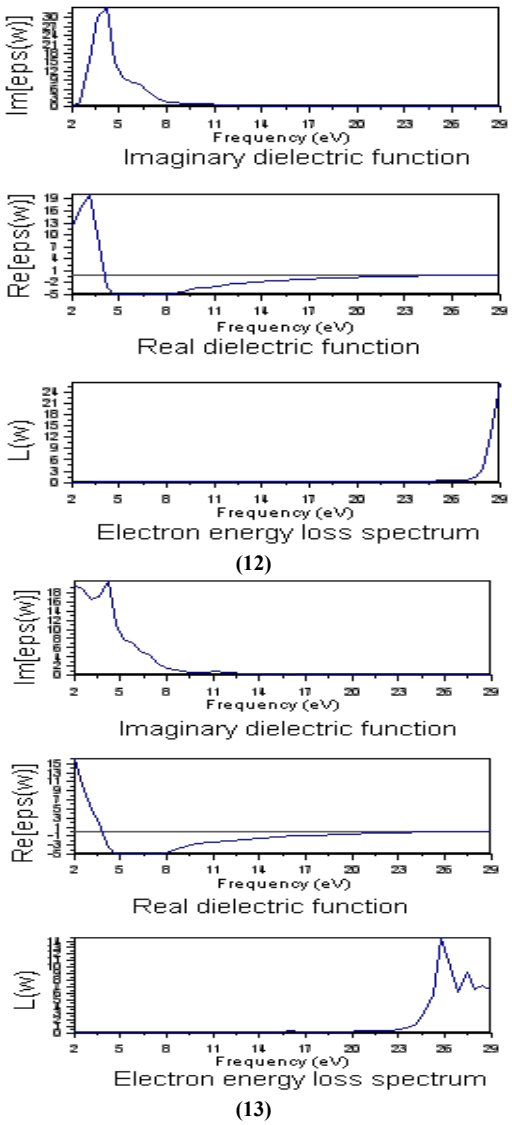

Figure 9. The calculated frequency dependent dielectric function and electron energy loss spectrum for Si(12) and Ge (13)

Calculated frequency dependent dielectric function and electron energy loss spectrum, of $Si_{025}Ge_{075}$ $Si_{075}Ge_{025}$, and $Si_{050}Ge_{050}$ are shown in figures 10(14) , figure 10(15) and figure 10(16), respectively.

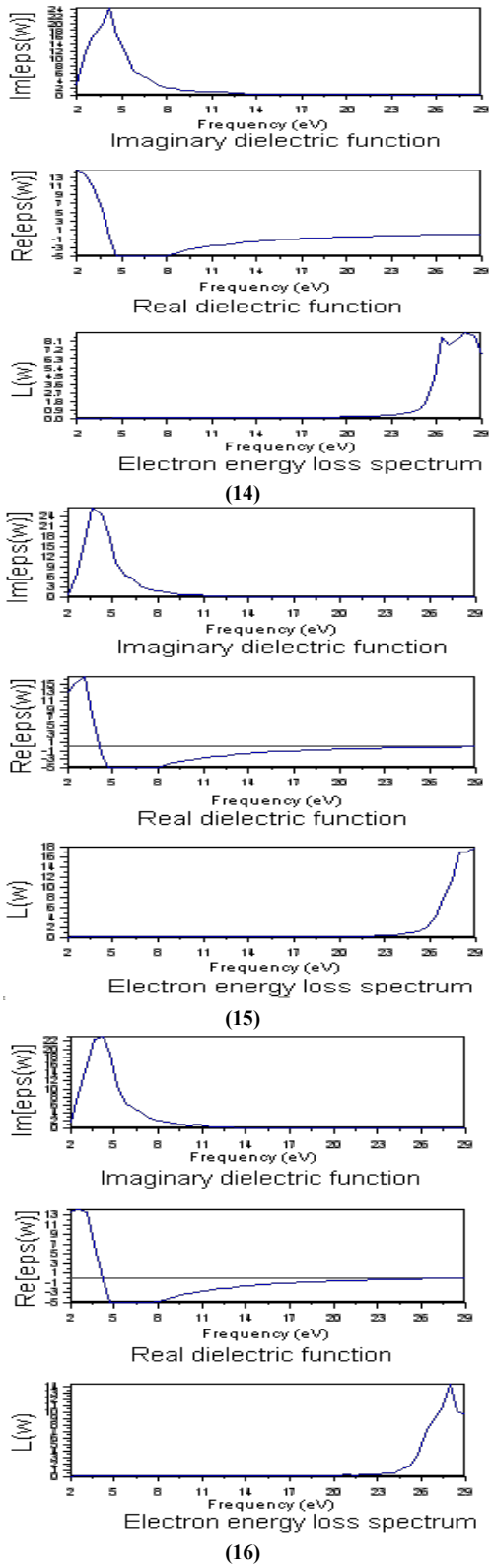

Figure 10. The calculated frequency dependent dielectric function and electron energy loss spectrum for $Si_{025}Ge_{075}$ (14), $Si_{075}Ge_{025}$ (15) and $Si_{050}Ge_{050}$

From these curves, one can state that the optical properties behaviors reveal that the indirect band gap transition is still present. The profiles for the imginary part of the dielectric function two peaks denoted by E1 and E2. We have

observed that the transition E2 is characterized by a rather broad peak and an amplitude more important than that of E1. The peak position of E2 is located at 4.5 eV but E1 is located near 2.2 eV (Fig.9(13)). For the silicon the profile of the εi exibits a net peak located near 4.3 eV (Fig. 9(12)).

The E2 peak appears to arise from a well-defined, limited region inside the Brillouin zone. Then it was interpreted as interband transitions at the X-point and along ∑-line, originating from transitions from the *p*-like states of the *sp*- hybridized conduction band in regions about the X- and K-points[32,33]. The low-energy peak at *E*1 was interpreted as interband transitions along the ΓL-line. For Si that is consistent with the transition energy of about 3.5 eV at theΓ-point[34]. Our calculations also show that the Si energy band gap along is fairly constant in k-space, which should result in strong absorption at this energy. The real part of the dielectric functions are also displayed in Figure 9 and Figure10. These profiles show a net peak up to the energy axis and a minimun below. Compared to the silicon, germanium exibits a richer spectrum. In the same figures we have also illustrated the electon energy loss spectrum. The structure in these spectra may be categorized into three distinct regions. For energy loss in the energy below 23 eV, the structure of the L(ω) arises from optical-like interband transitions. The incident electron loss energy by scattering off a valence electron which is promoted into the conduction band. In the 23-30 eV region, the value of L(ω) is large with a net peak leading to state that the dominates process in this region is plasmon excitation. The third region is thought to arise from excitation in which the energy loss by the scattered electron is used to promote a core electron. The effect of increasing the germanium composition is clearly seen. We notice that position peaks were shifted to the left. We have also observed that not only the optical transition *E*1 peak was reduced but it tends to disappear and to form with E2 only a single broad peak centered around 4.3 eV.

These all optical properties results agree very well with other theoretical as well as the experimental results[35-38]. The polarity of the Si-Ge bond can with reasonable accuracy be neglected, which means that the zero-frequency transverse optical and longitudinal optical modes are degenerate.

4. Conclusions

We have made a detailed investigation of the electronic structure and optical properties of Si, Ge and $Si_{1-x}Ge_x$ alloy using the full-potential linear muffin-tin orbital (FP- LMTO) augmented with the plane wave approximation (PLW). The effect of the approximation to the exchange-correlation energy were treated by the local density approximation (LDA). From the simulation results, it is found that the theoretical ground-state parameters, the band structure, the density of states (DOS), the chemical bonding and the optical properties agree quite well with experimental information as well other theoretical works. In the present work, we have also checked the transferability of the considered calculation method to predict the structural, electronic and optical properties for $Si_{1-x}Ge_x$ alloy from those of their parent semiconductors. Finally, one can deduced from these results that the weakly straind G-rich SiGe layers possess very promising properties for both electronic and optical applications. Further work is in progress.

REFERENCES

[1] J.C. Phillips, *Bonds and Bands in Semiconductors*. Academic Press, New York (1973)

[2] A.R. Jivani, P.N. Gajjar and A.R. Jani, *Semiconductor Physics, Quantum Electronics and Optoelectronics* 5, (2002) p. 243-246

[3] T. Soma, *Phys. status solidi* (b), 95, (1979) p. 427-431

[4] S. Gonazalez, Empirical pseudopotential method for the band structure calculations of strained silicon germanium materials. *Ph. D. Thesis, Arizona State University,* Arizona, 2001

[5] C.J. Williams, Impact ionization and Auger recombination in SiGe heterostructures. Ph. D. Thesis, University of Newcastle, Tyne, 1996

[6] H.G.Grimmeiss,Semicond. 33, (1999) 939. U. Koing et al., Proc.Conf. High Speed Semicond. Devices and Circuits,p.14 (IEEE), Cornell, 1997); H. Temkin, et al. Appl. Phys. L ETT.52, (1988) 1089; S.C. Jain, al, Semicond.Sci. Technol. 16,R 51 (2001);ibid,R76 (2001)

[7] Al-Sameen T. Khan, PR. Berger, F. J. Guarin, and S. S. Iyer, Thin Solid Films, 294, (1997) 122-124.

[8] F. Chen, B. A. Orner, D. Guerin, A. Khan, P. R. Berger, S. I. Shah, and J. Kolodzey, IEEE Electon Device Letters, 17, (1996) 589-591

[9] X. Shao, S. L. Rommel, B. A. Orner, P. R. Berger, J. Kolodzey, and K. M. Unruh, IEEE Electron Device Letters, 18, (1997) 7-9

[10] A. T. Khan, P. R. Berger, F. J. Guarin, and S. S. Iyer, Applied Physics Letters, 68, (1996) 3105-3107

[11] D. K. Nayak, et al. IEEE Electron Divice Lett. 12,154 (1991); S. Lluryi. Et al . IEEE Trans. Electron Devices 31. (1984) 1135; TP. Pearsall et al. IEEE Electron Device Lett. 7, (1986) 308

[12] S. Y. Savrasov, Phys. Rev. B 54 , (1996) 16470

[13] S. Savrasov, D. Savrasov, Phys. Rev. B 46 (1992) 12181

[14] D. Rached, M. Rabah, N. Benkhettou, M. Driz and B. Soudini Physica B : Physics of Condensed Matter, 337/1-4 (2003) pp. 394-403

[15] O. K. Andersen, Phys. Rev. B 12, (1975) 3060

[16] H. L. Skriver, *The LMTO Method*, Springer-Verlag (1984).

[17] O. K. Andersen and O. Jepsen, Phys. Rev. Lett. 53, (1984) 2571

[18] O. K. Andersen, Z. Pawlowska, and O. Jepsen, Phys. Rev. B 34, (1986) 5253

[19] P. Vogl, H.P. Hjalmarson, and J.D. Dow, J. Phys. Chem. Solids 44, 365 (1983)

[20] P. Blochl, O. Jepsen, and O.K. Andersen, Phys. Rev. B 49 , (1994) 16223

[21] B. Van Zeghbroeck, Chapter 2: Semiconductor Fundamentals(2007)

[22] *Semiconductor Basic Data*, ed. by O. Madelung (Springer, Berlin, 1996)

[23] J. S. Faulkner, Prog. Mater. Sci. 27, (1982)3

[24] S. van Teeffelen, C. Persson, O. Eriksson and B. Johansson, J. Phys.: Conden. Matter 15, (2003) 489

[25] C. Persson, O. Nur, M. Willander, E. A. de Andrada e Silva, and A. Ferreira da Silva, *Brazilian* Journal of Physics, vol. 36, no. 2A, (2006) 447

[26] P. Hohenberg, W. Kohn, Phys. Rev. B 136 (1964) 864

[27] W. Kohn, L.J. Sham, Phys. Rev. A 140 (1965) 1133

[28] J. R. Chelikovsky, M. L. Cohen , Phys. Rev. B14, 556 (1976)

[29] Alouani M, Koch J M and Khan M A *J. Phys*. F16 (1986) 437

[30] Koenig C and Khan M A *Phys. Rev.* B17 (1983) 6129

[31] Khan M A, Kashyap A, Solanki A K, Nautiyal T and Auluck S *Phys. Rev.* B48 (1993)16947

[32] R. Ahuja *et al*., J. Appl. Phys. 93, (2002) 3832

[33] P. Lautenschlager *et al*, Phys. Rev. B 36, (1987) 4821

[34] Humlicek *et al*., J. Appl. Phys. 65, (1989) 2827

[35] R. K. Schaevitz, J. E. Roth, S.n Ren, O. Fidaner, and D. B. Miller, IEEE JOURNAL OF SELECTED TOPICS IN QUANTUM ELECTRONICS, VOL. 14, NO. 4, JULY/AUGUST 2008

[36] O. Arbouche, B. Belgoumène, B. Soudini, Y. Azzaz, H. Bendaoud and K. Amara, Comp. Mat. Sc. Vol. 47, Issue 3, January (2010), 685-692

[37] K. Schwarz, P. Blaha, S. Trickey, Molecular Physics (invited), 108 (2010), 3147 - 3166

[38] G. Pizzi, M. Virgilio and G. Grosso *Nanotechnology* 21 (2010) 055202